Carbon 119 (2017) 446–452

Contents lists available at ScienceDirect

Carbon

journal homepage: www.elsevier.com/locate/carbon

Modeling of spectral shift in Raman spectroscopy, photo- and electro-luminescence induced by electric field tuning of graphene related electronic devices

Ling-Feng Mao [a, *], Jue Wang [b, **], L. Li [a], H. Ning [a], Changjun Hu [a, ***]

[a] School of Computer & Communication Engineering, University of Science & Technology Beijing, 30 Xueyuan Road, Haidian District, Beijing, 100083, PR China

[b] Computer Network Information Center of CAS, Beijing, 100190, PR China

ARTICLE INFO

Article history:
Received 14 March 2017
Received in revised form
28 April 2017
Accepted 28 April 2017
Available online 28 April 2017

ABSTRACT

The continuous tuning of the emission (absorption) spectra of the excitons in graphene field-effect transistors by the gate (drain) voltage is of great technological significance. And its physical mechanism still remains to be unraveled. A new physical model of the electric field dependent exciton energy and its impacts on the emission (absorption) spectra is proposed based on the ambipolar transport theory with the energy balance assumption. By comparing the shift in the emission (absorption) peak predicted by the proposed model with those experimental data reported in the literature, we could conclude that the energy relaxation of the excitons plays a dominant role in the spectral shift. Thus, the energy relaxation of the excitons is a physical origin for the gate (drain) voltage dependent spectral shift. The proposed model predicates that the gate control of the spectral shift depends on the channel length, the gate oxide thickness, the dielectric constant of the gate oxide, the thickness of the graphene layer, and the dielectric constant of the graphene, whereas the drain control of the spectral shift is mainly determined by the channel length. These findings will benefit to better understand the effect of the electric field on the emission (absorption) spectrum.

1. Introduction

A single layer of honeycomb carbon lattice is called as graphene, which has the properties of zero band gap and linear energy-momentum relation due to its two-dimensional nature. Optical spectroscopies can be used to probe its electronic excitations and excited-state properties [1]. A large class of monolayer materials exhibit emergent photoluminescence [2]. Photoluminescence (absorption of light) leads to the creation of the bound electron-hole pairs (excitons), whereas electroluminescence (emission of light) leads to recombination of electrically injected electron-hole pairs [3]. Hot-electron luminescence has been demonstrated [4]. The electrostatic tunability of optical transitions in graphene or other monolayer semiconductor has been reported [5,6]. However, using electrostatic gating to control optic transitions is still a challenge because its physical mechanism still remains not to be fully explained. By applying a vertical electric field, the emission energy of the luminescence in a two-dimensional material can be tuned more than 1 meV [7]. Here we achieve the goal how to physically understand gate-variable optical transitions.

The energy relaxation of channel electrons could be a physical origin for the current-collapse phenomenon in the AlGaN/GaN high-electron mobility transistors [8], might have a large effect on the gate leakage current in the graphene field-effect transistors [9], and could largely impact on the effective activation energy in the organic semiconductors [10]. These papers demonstrate that the performance of semiconductor devices could be largely affected by the energy relaxation of carriers. Thus, it is worth studying the energy relaxation of exciton (electron-hole pair) under an applied electric field and its impacts on the absorption and emission of light in semiconductor devices.

The purpose of this paper is to shed some light on how an applied electric field impacts on the absorption and emission of light with the help of the ambipolar transport of exciton under the

* Corresponding author.
** Corresponding author.
*** Corresponding author.
E-mail addresses: lingfengmao@ustb.edu.cn (L.-F. Mao), wangjue@sccas.cn (J. Wang), huchangjun@ies.ustb.edu.cn (C. Hu).

http://dx.doi.org/10.1016/j.carbon.2017.04.070
0008-6223/

energy balance (energy relaxation) in the devices physics. In particular, an analytical physical model to describe the shift in the absorption and emission spectral shape in the graphene field-effect transistors is proposed. Such a model can be applied to explain the experimental relation between the shift in the absorption and emission spectral shape and the physical parameters of the graphene related electronic devices such as the gate voltage, the drain voltage, the channel length, and etc. The proposed model clearly demonstrates a physical origin of the peak shift in the absorption and emission spectra through its simplicity and analytic nature. The proposed model states that the electric field dependent spectral shifts can be modulated by changing physical parameters of graphene related electronic devices. This proposed model is by virtue of its physical simplicity and important practical value.

2. Theory

The continuity equations for electron and hole particle fluxes can be written as [11]

$$-\nabla\cdot\vec{J}_{p-p}-\frac{p}{\tau_p}+g_0+g'=\frac{\partial p}{\partial t} \tag{1}$$

$$-\nabla\cdot\vec{J}_{p-n}-\frac{n}{\tau_n}+g_0+g'=\frac{\partial n}{\partial t} \tag{2}$$

where τ_p is the hole lifetime, τ_n is the electron lifetime, g_0 is the equilibrium generation of electron-hole pairs, g' is the generation rate of electron-hole pairs in excess of equilibrium, p is the hole density, n is the electron density.

Electron and holes in electron-hole pairs (excitons) move dependently each other with the same lifetime, drift mobility and diffusion coefficient. Thus an electron-hole pair can be treated as a quasi-particle. Thus, the electrical current density in a semiconductor is

$$J=J_p+J_n=q\left(\mu_p p+\mu_n n\right)E+q\left(D_n\frac{\partial n}{\partial x}-D_p\frac{\partial p}{\partial x}\right) \tag{3}$$

$$J_p=q\mu_p pF-qD_p\frac{\partial p}{\partial x} \tag{4}$$

$$J_n=q\mu_n nF+qD_n\frac{\partial n}{\partial x} \tag{5}$$

where F is the electric field. Therefore, the particle flux can be obtained as

$$J_{p-p}=\frac{J_p}{q}=\mu_p pF-D_p\frac{\partial p}{\partial x} \tag{6}$$

$$J_{n-n}=\frac{J_n}{-q}=-\mu_n nF-D_n\frac{\partial n}{\partial x} \tag{7}$$

The continuity equations for holes and electrons (Eqs. (1) and (2)) can be rewritten as

$$-\mu_p\frac{\partial(pF)}{\partial x}+D_p\frac{\partial^2 p}{\partial x^2}-\frac{p}{\tau_p}+g_0+g'=\frac{\partial p}{\partial t} \tag{8}$$

$$\mu_n\frac{\partial(nF)}{\partial x}+D_n\frac{\partial^2 n}{\partial x^2}-\frac{n}{\tau_n}+g_0+g'=\frac{\partial n}{\partial t} \tag{9}$$

Note that the excitons (electron-hole pairs) generate and recombine together (it requires that $\tau_p=\tau_n=\tau$), thus the electron density and hole density in a semiconductor can be written as

$$p-p_0=\Delta p=\Delta n=n-n_0 \tag{10}$$

where n_0 is the electron density in the equilibrium state, p_0 is the hole density in the equilibrium state, Δn (Δp) is the exciton density. And

$$-\mu_p F\frac{\partial(\Delta p)}{\partial x}-\mu_p\Delta p\frac{\partial(F)}{\partial x}+D_p\frac{\partial^2\Delta p}{\partial x^2}-\frac{\Delta p}{\tau}+g_0+g'=\frac{\partial\Delta p}{\partial t} \tag{11}$$

$$\mu_n E\frac{\partial(\Delta n)}{\partial x}+\mu_n\Delta n\frac{\partial(F)}{\partial x}+D_n\frac{\partial^2\Delta n}{\partial x^2}-\frac{\Delta n}{\tau}+g_0+g'=\frac{\partial\Delta n}{\partial t} \tag{12}$$

The current density is

$$\begin{aligned}J&=J_p+J_n\\&=q\left(\mu_p p_0+\mu_n n_0+\mu_p\Delta p+\mu_n\Delta n\right)F+q\left(D_n\frac{\partial\Delta n}{\partial x}-D_p\frac{\partial\Delta p}{\partial x}\right)\end{aligned} \tag{13}$$

The above equation (Eq. (13)) demonstrates that both electrons and holes in excitons (electron-hole pairs) give their contribution to the current density. And its contribution to the current density can be divided into two parts: one is for the drift current, and the other is for the diffusion current.

After excitons (electron-hole pairs) are generated, there are many processes (for example, thermalization, energy relaxation, and recombination) that will occur. In this article, we focus on the energy relaxation of the excitons (electron-hole pairs). The energy conservation equation in a semiconductor device can be written as [12]

$$\begin{aligned}\frac{\partial T_p}{\partial t}+\nabla\left(v_p T_e\right)&=\frac{1}{3}T_p\nabla v_p+\frac{2}{3nk_B}\nabla\left(\kappa_p\nabla T_p\right)-\frac{T_p-T_L}{\tau_{e-p}}\\&\quad+\frac{m_p^* v_p^2}{3k_B}\left(\frac{2}{\tau_{m-p}}-\frac{1}{\tau_{e-p}}\right)\end{aligned} \tag{14}$$

$$\begin{aligned}\frac{\partial T_n}{\partial t}+\nabla\left(v_n T_n\right)&=\frac{1}{3}T_n\nabla v_n+\frac{2}{3nk_B}\nabla\left(\kappa_n\nabla T_n\right)-\frac{T_n-T_L}{\tau_{e-n}}\\&\quad+\frac{m_n^* v_n^2}{3k_B}\left(\frac{2}{\tau_{m-n}}-\frac{1}{\tau_{e-n}}\right)\end{aligned} \tag{15}$$

where $\tau_{m\text{-}p}$ ($\tau_{m\text{-}n}$) is the momentum relaxation time of holes (electrons), $\tau_{e\text{-}p}$ ($\tau_{e\text{-}n}$) is the energy relaxation time of holes (electrons), v_p (v_n) is the hole (electron) velocity, T_L is the lattice temperature (device temperature), T_p (T_n) is the hole (electron) temperature, m_p^* (m_n^*) is the effective mass of holes (electrons), k_B is the Boltzmann constant, and κ_n is the thermal conductivity of electron. Neglecting the space distribution, the above equation (Eqs. (14) and (15)) at a given point in a semiconductor can be rewritten as

$$\frac{\partial T_p}{\partial t}=-\frac{T_p-T_L}{\tau_{e-p}}+\frac{m_p^* v_p^2}{3k_B}\left(\frac{2}{\tau_{m-p}}-\frac{1}{\tau_{e-p}}\right) \tag{16}$$

$$\frac{\partial T_n}{\partial t}=-\frac{T_n-T_L}{\tau_{e-n}}+\frac{m_n^* v_n^2}{3k_B}\left(\frac{2}{\tau_{m-n}}-\frac{1}{\tau_{e-n}}\right) \tag{17}$$

Under a low constant electric field, the drift velocity of holes and electrons can be written as [13]

$$v_p = \mu_p E = \frac{q\tau_{m-p}}{m_p^*}F \tag{18}$$

$$v_n = \mu_n E = \frac{q\tau_{m-n}}{m_n^*}F \tag{19}$$

For a stead sate condition ($\frac{\partial \Delta p}{\partial t} = 0$), and an assumption that the excitons are in thermal equilibrium,

$$T_p - T_L = \frac{m_p^* v_p^2}{3k_B}\tau_{e-p}\left(\frac{2}{\tau_{m-p}} - \frac{1}{\tau_{e-p}}\right) \tag{20}$$

$$T_n - T_L = \frac{m_n^* v_n^2}{3k_B}\tau_{e-n}\left(\frac{2}{\tau_{m-n}} - \frac{1}{\tau_{e-n}}\right) \tag{21}$$

Usually, the energy relaxation time is much larger than the momentum relaxation time [14–16]. Thus, Eq. (20) and Eq. (21) can be approximate as

$$E_p = \frac{3k_B(T_p - T_L)}{2} = m_p^* v_p^2 \frac{\tau_{e-p}}{\tau_{m-p}} = q\mu_p \tau_{e-p} F^2 \tag{22}$$

$$E_n = \frac{3k_B(T_n - T_L)}{2} = m_n^* v_n^2 \frac{\tau_{e-e}}{\tau_{m-e}} = q\mu_n \tau_{e-n} F^2 \tag{23}$$

The above equations imply that excitons (electron-hole pairs) can get a kinetic energy from the applied electric field, and thus the corresponding kinetic energy can be written as

$$E_{2-F} = E_2 + q\mu_n \tau_{e-n} F^2 \tag{24}$$

$$E_{1-F} = E_1 + q\mu_p \tau_{e-p} F^2 \tag{25}$$

$$E_{ex-F} = E_{ex} + q\left(\mu_p \tau_{e-p} + \mu_n \tau_{e-n}\right)F^2 \tag{26}$$

where E_2, E_1, E_{ex} are the electron energy, the hole energy in an electron-hole pair, and the energy of the exciton without applied electric field, respectively. In other words, the binding energy of an exciton under an applied electric field at a temperature will be written as

$$E_B = E_{B0} - q\left(\mu_p \tau_{e-p} + \mu_n \tau_{e-n}\right)F^2 - \frac{3}{2}k_B T_L \tag{27}$$

The drift velocity of electrons and holes under a high electric field can be obtained as [17]

$$v_p = \frac{\mu_{p0}F}{1 + \mu_{p0}F/v_{psat}} = \frac{1}{\frac{1}{\mu_{p0}F} + \frac{1}{v_{psat}}} \tag{28}$$

$$v_n = \frac{\mu_{n0}F}{1 + \mu_{n0}F/v_{psat}} = \frac{1}{\frac{1}{\mu_{n0}F} + \frac{1}{v_{nsat}}} \tag{29}$$

Then, the binding energy of an exciton can be written as

$$E_B = E_{B0} - \frac{1}{2}\left[m_p\left(\frac{1}{\mu_{p0}F} + \frac{1}{v_{psat}}\right)^{-2} + m_n\left(\frac{1}{\mu_{n0}F} + \frac{1}{v_{nsat}}\right)^{-2}\right] - \frac{3}{2}k_B T_L \tag{30}$$

The stimulated emission rate per unit volume is determined by the transition probability, the electron density, the hole density, and the photon density [18],

$$R = \frac{A_{21}}{Z(E_{21})} n_{ph}(E_{21})\rho_C(E_2 - E_1)\rho_V(E_2 - E_1)[f_2 - f_1] \tag{31}$$

$$f_1 = \frac{1}{\exp[(E_1 - E_{Fv})/k_B T] + 1} \tag{32}$$

$$f_2 = \frac{1}{\exp[(E_2 - E_{Fc})/k_B T] + 1} \tag{33}$$

$$E_{Fv} = E_v - k_B T \ln\left(\frac{p}{N_v}\right) \tag{34}$$

$$E_{Fc} = E_c + k_B T \ln\left(\frac{n}{N_c}\right) \tag{35}$$

$$n_{ph}(E_{21}) = \frac{8\pi n_r^3 E_{21}^2}{h^3 c^3 \exp[E_{21}/(k_B T)] - h^3 c^3} \tag{36}$$

$$A_{21} = \frac{4\pi q^2 n_r E_{21}}{m^2 \varepsilon_0 h^2 c^3}\left|\langle 1|\hat{p}|2\rangle\right|^2 \tag{37}$$

$$Z(E_{21}) = \frac{A_{21}}{B} \tag{38}$$

$$B = \frac{q^2 h}{2m^2 \varepsilon_0 n_r^2 E_{21}}\left|\langle 1|\hat{p}|2\rangle\right|^2 \tag{39}$$

n_r is the effective refractive index, ρ_c $(E_2 - E_c)$ is the density of states, h is Planck's constant, m is the electron mass, E_c is the energy of the bottom of the conduction band, E_v is the top of the valence band, p is the momentum operator, E_{21} is the photon energy, N_c is the effective density of states for the electrons, N_v is the effective density of states for the electrons the holes, ε_0 is permittivity in a vacuum, c is the speed of light in a vacuum, $\langle 1|$ is the wave functions of the valence band, and $|2\rangle$ is the wave functions of the conduction band. According to Eqs. (24) and (25), we can obtain that $E_{21-F} = E_{21} + q(\mu_p \tau_{e-p} + \mu_n \tau_{e-n})F^2$. With the assumption that optical transitions have an energy width of $\hbar/\tau_{in}$ (τ_{in} the relaxation time due to electron scatterings and transitions), the spectral shape of Lorentzian [18]

$$L(E_{21}) = \frac{1}{\pi}\frac{\hbar/\tau_{in}}{(E_{21} - E)^2 + (\hbar/\tau_{in})^2} \tag{40}$$

According to Eqs. (27), (30), and (40), we can predict that how an applied electric field impacts on the spectral shape of the absorption and emission spectra in graphene related electronic devices.

3. Results and discussion

Fig. 1 shows that the absorption and emission process in a graphene or other materials. Here $|0\rangle$ is the ground state, and $E_1 + \frac{\hbar K^2}{2M}$ is the excited state. Note that the kinetic energy ($\frac{\hbar K^2}{2M}$) in the excited states equals the decrease in the binding energy of an exciton under an applied electric field, which is $q(\mu_p \tau_{e-p} + \mu_n \tau_{e-n})F^2$ according to Eq. (27). Thus the absorption and emission spectrum in a graphene or other materials depends on the square of the applied electric field. In the following, we will discuss how an applied gate voltage and drain voltage in a graphene related

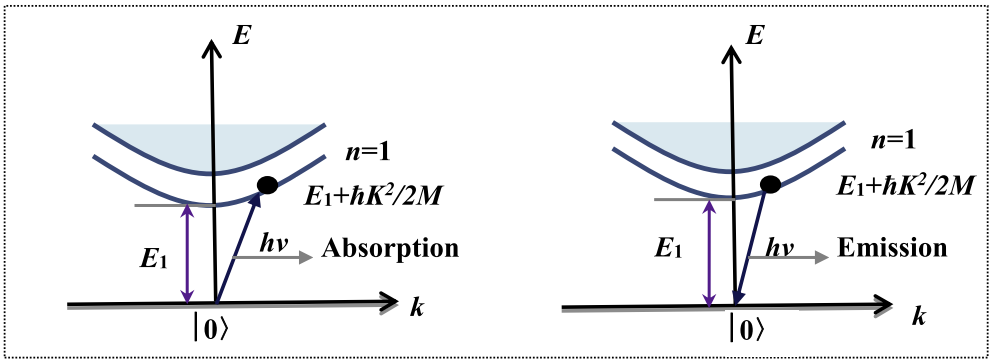

(a) (b)

Fig. 1. Two-particle (electron-hole pair) picture of one photon absorption (a) and emission (b). (A colour version of this figure can be viewed online.)

field-effect transistors impacts on the channel electric field.

The maximum electric field in the channel based on a two dimension analytical model by reducing a 2-D (two dimensional) electrostatic problem to a 1-D (one dimensional) case can be written as is [19,20]

$$F_m = F(0) = C_1 V_{DS} + C_2 V_{GS} + C_3 \tag{41}$$

where C_1, C_2, and C_3 are just fitting parameters for field-effect transistors. Note that $C_1 = \frac{-2}{\lambda(e^{L/\lambda} - e^{-L/\lambda})}$, and $C_2 = \frac{2-(e^{L/\lambda}+e^{-L/\lambda})}{\lambda(e^{L/\lambda}-e^{-L/\lambda})}$, here $\lambda = \sqrt{\frac{\varepsilon_s t_s t_{ox}}{\varepsilon_{ox}}}$, L is the channel length, t_{ox} is the gate oxide thickness, t_s is the graphene layer thickness, ε_{ox} is the dielectric constant of the gate oxide, and ε_s is the dielectric constant of the graphene. If we consider a first order approximation, we can obtain that $e^{\frac{L}{\lambda}} - e^{-\frac{L}{\lambda}} \approx 2L/\lambda$, and $e^{\frac{L}{\lambda}} + e^{-\frac{L}{\lambda}} \approx 2 + 2(L/\lambda)^2$. Therefore, $C_1 \approx -\frac{1}{L}$, and $C_2 \approx -\frac{L}{\lambda^2}$. Eq. (41) can be rewritten as

$$F = |F_m| = |F(0)| = \begin{cases} \frac{1}{L}V_{DS} + \frac{L}{\lambda^2}V_{GS} - C_3 & C_3 \le \frac{1}{L}V_{DS} + \frac{L}{\lambda^2}V_{GS} \\ C_3 - \frac{1}{L}V_{DS} - \frac{L}{\lambda^2}V_{GS} & C_3 \ge \frac{1}{L}V_{DS} + \frac{L}{\lambda^2}V_{GS} \end{cases} \tag{42}$$

According to Eqs. (24) and (25), $h\nu_1 = E_{21-F} = E_{21} + q(\mu_p\tau_{e-p} + \mu_n\tau_{e-n})F^2$, and $h\nu_0 = E_{21}$. Therefore, $h(\nu_1 - \nu_0) = q(\mu_p\tau_{e-p} + \mu_n\tau_{e-n})F^2$, Then, we can obtain

$$h(\nu_1 - \nu_0) = q\left(\mu_p\tau_{e-p} + \mu_n\tau_{e-n}\right) \times \begin{cases} \left(\frac{1}{L}V_{DS} + \frac{L}{\lambda^2}V_{GS} - C_3\right)^2 & C_3 \le \frac{1}{L}V_{DS} + \frac{L}{\lambda^2}V_{GS} \\ \left(C_3 - \frac{1}{L}V_{DS} - \frac{L}{\lambda^2}V_{GS}\right)^2 & C_3 \ge \frac{1}{L}V_{DS} + \frac{L}{\lambda^2}V_{GS} \end{cases} \tag{43}$$

$$\sqrt{h(\nu_1 - \nu_0)} = \sqrt{q\left(\mu_p\tau_{e-p} + \mu_n\tau_{e-n}\right)} \times \begin{cases} \frac{1}{L}V_{DS} + \frac{L}{\lambda^2}V_{GS} - C_3 & C_3 \le \frac{1}{L}V_{DS} + \frac{L}{\lambda^2}V_{GS} \\ C_3 - \frac{1}{L}V_{DS} - \frac{L}{\lambda^2}V_{GS} & C_3 \ge \frac{1}{L}V_{DS} + \frac{L}{\lambda^2}V_{GS} \end{cases} \tag{44}$$

The above equations denote that the relation between the absorption (emission) frequency and the source-drain voltage (source-gate voltage) is a second degree polynomial equation. Note that a shorter channel length leads to a larger shift in the peak position in the absorption and emission spectra when the source-drain voltage increases in a graphene related field-effect transistor, whereas a shorter channel length leads to a smaller shift in the peak position in the absorption and emission spectra when the source-gate voltage increases. At the same time, the correlation between the peak position and the source-drain voltage is only affected by the channel length. But the gate oxide thickness, the dielectric constant of the gate oxide, the thickness of the graphene layer, and its dielectric constant have impacts on the correlation between the peak position and the source-gate voltage.

Fig. 2 clearly show how the peak position (frequency) of electroluminescence in the all-graphene-based field-effect LED (light-emitting diode) is affected by the gate voltage. A second-order polynomial function can described the gate voltage dependence of the peak position (wavelength) well. Experimental data in Fig. 2 come from Fig. 2 in Ref. [21]. Note that the Adj. R-Square is the adjusted coefficient of determination in statistics, which can tell one what percent of the total variability is accounted for by the model. Thus, it is used for statistical description for goodness of fitting, and the fitting process is one hundred percent successful when the value of the Adj. R-Square is 1. The value of the Adj. R-Square for the fitting in the Fig. 2 is 0.97678, it means that the propose model is valid to describe electroluminescence in the all-graphene-based field-effect LED because the value is close to 1. Additionally, the fitting parameter C_2 is $2.73*10^{-6} \times \frac{hc}{q(\mu_p\tau_{e-p}+\mu_n\tau_{e-n})}$ because we did not know the exact value of electron mobility and hole mobility.

Fig. 3 depicts how the gate voltage impacts on the Raman peak A_{1g} in monolayer MoS_2/graphene heterostructures. Experimental data in Fig. 3 come from Fig. 4 in Ref. [22]. The value of Adj. R-Square for the fitting in the Fig. 3 is 0.98469. This also means that the proposed model agrees well with the experimental conclusions. The fitting parameter C_2 is $6.29 \times \frac{hc}{q(\mu_p\tau_{e-p}+\mu_n\tau_{e-n})}$.

Fig. 4 demonstrates how the Raman shifts of both G-band and 2D-band in back-gated graphene field effect transistors is influenced by the gate voltage. Experimental data in Fig. 4 come from Fig. 2c in Ref. [23]. The values of the Adj. R-Square for the fitting G-band and 2D-band curves in the Fig. 4 are 0.98939 and 0.9843, respectively. This also means that the proposed model agrees well with the experimental results. The fitting parameters C_2 for G-band and 2D-band bands are $-3.94 \times 10^{-2} \times \frac{hc}{q(\mu_p\tau_{e-p}+\mu_n\tau_{e-n})}$, and $-1.01 \times 10^{-2} \times \frac{hc}{q(\mu_p\tau_{e-p}+\mu_n\tau_{e-n})}$, respectively.

Fig. 5 gives how the E_{33}-exciton in the resonance Raman excitation spectrum (RBM, Stokes transition) of the semiconducting carbon nanotube depends on the gate voltage. Experimental data in

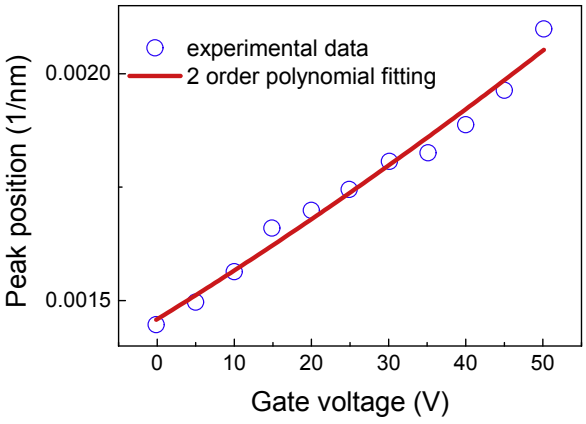

(a)

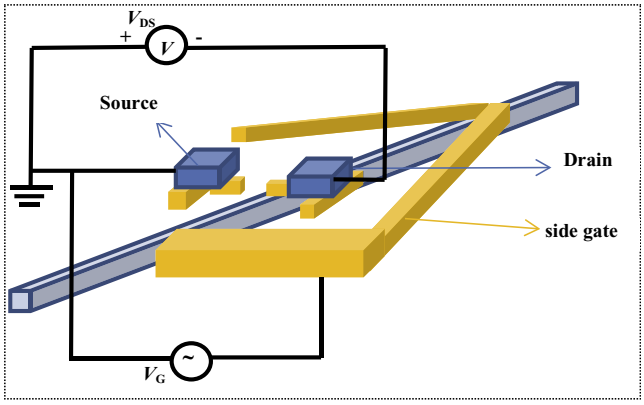

(b)

Fig. 2. (a) The peak position (frequency) in the electroluminescence spectrum as a function of the gate voltage for the all-graphene-based field-effect light-emission-device, (b) The schematic of the graphene field-effect LED and the electroluminescence property measurement. (A colour version of this figure can be viewed online.)

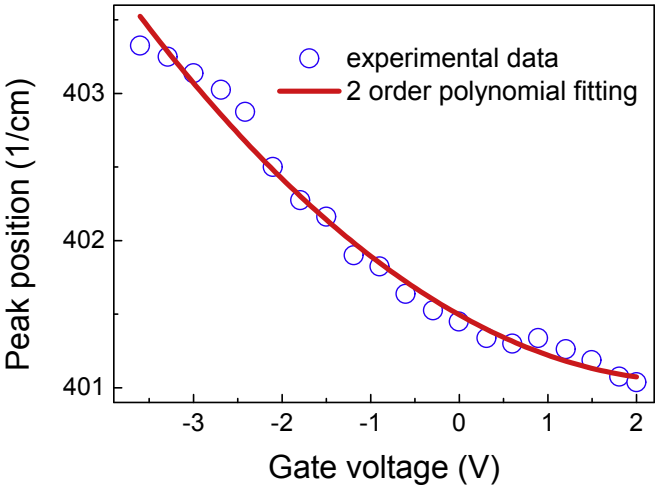

Fig. 3. The peak position (A_{1g}) in the Raman spectra as a function of the gate voltage for the MoS_2/graphene heterostructures devices. (A colour version of this figure can be viewed online.)

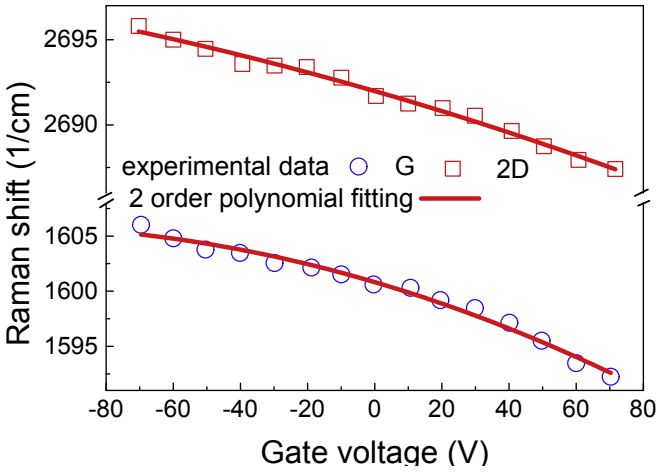

Fig. 4. The shift in the peak position in the Raman spectrum as a function of the gate voltage for the back-gated graphene field effect transistors. (A colour version of this figure can be viewed online.)

Fig. 5 come from Fig. 3b in Ref. [24]. This figure clearly demonstrates that the proposed model agrees well with the experimental data. The fitting parameter C_2 is $-1.26 \times 10^{-3} \times \frac{hc}{q(\mu_p \tau_{e-p} + \mu_n \tau_{e-n})}$.

Fig. 6 shows how the source-drain voltage impacts on the E_{11} peak energy in the measured photoluminescence of the partially suspended carbon nanotube field-effect transistors. Experimental data in Fig. 6 come from Fig. 3 in Ref. [25]. This figure further demonstrates that the proposed model agrees well with the experimental data. The fitting parameter C_1 is $-8.07 \times 10^{-4} \times \frac{hc}{q(\mu_p \tau_{e-p} + \mu_n \tau_{e-n})}$.

Fig. 7 shows how the 2D-band peak frequency in Raman spectra of electrostatically gated single-layer graphene during the first heating cycles is affected by the gate voltage. Experimental data in Fig. 7 come from Fig. 8 in Ref. [26]. This figure also shows that correlation between the peak energy in the absorption spectrum and the gate voltage obeys a 2 order polynomial relation that is predicted by the proposed model. The fitting parameters C_1 at the temperature of 298 K, 387 K, 471 K and 550 K are $1.27 \times 10^{-3} \times \frac{hc}{q(\mu_p \tau_{e-p} + \mu_n \tau_{e-n})}$, $2.14 \times 10^{-3} \times \frac{hc}{q(\mu_p \tau_{e-p} + \mu_n \tau_{e-n})}$,

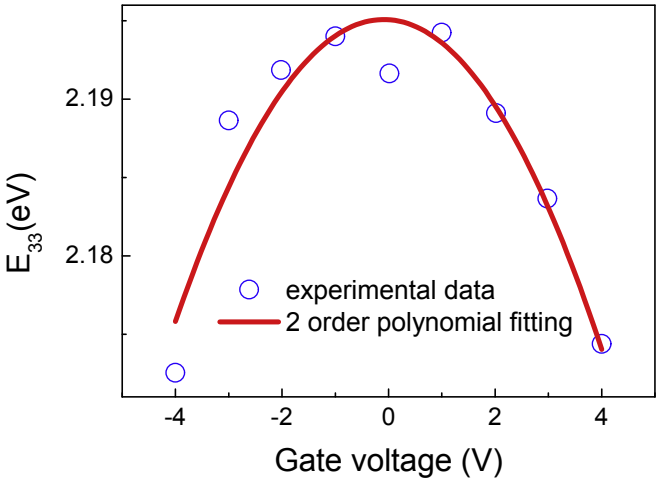

Fig. 5. The E_{33} peak energy in the resonance Raman excitation spectrum as a function of the gate voltage for the carbon nanotube field-effect transistors. (A colour version of this figure can be viewed online.)

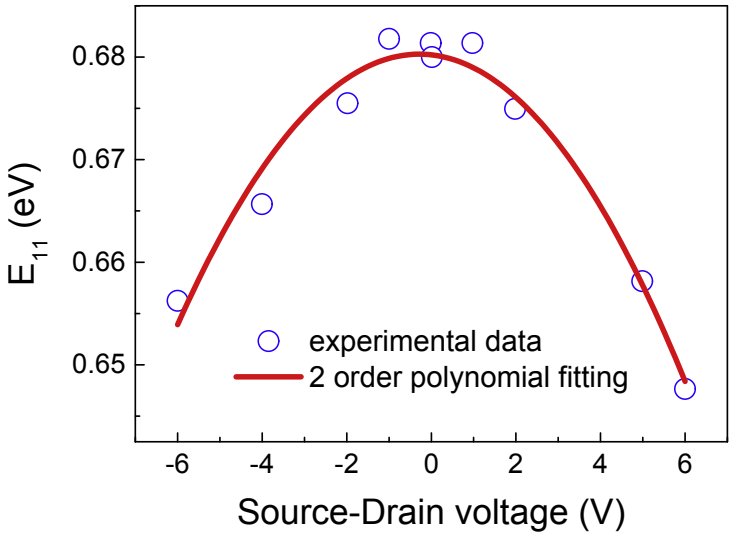

Fig. 6. The E_{11} peak energy in the measured photoluminescence band as a function of the source-drain voltage for the partially suspended carbon nanotube field-effect transistors. (A colour version of this figure can be viewed online.)

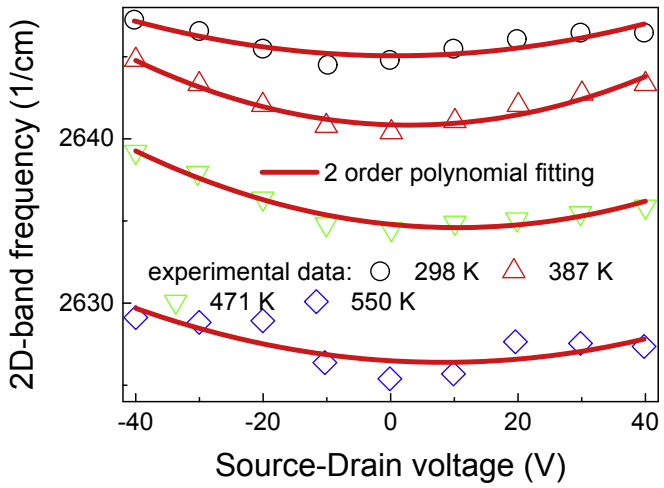

Fig. 7. The 2D-band frequency in the Raman spectrum during the first heating cycles as a function of the source-drain voltage for the electrostatically gated single-layer graphene. (A colour version of this figure can be viewed online.)

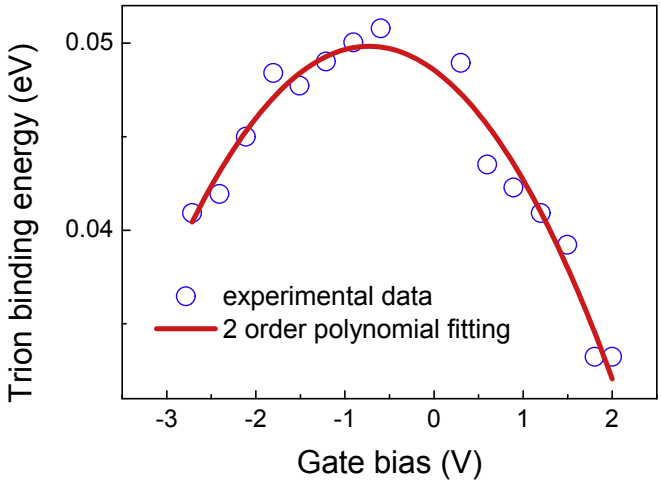

Fig. 8. The trion binding energy in the photoluminescence spectrum as a function of the source-drain voltage for the MoS_2/Graphene heterostructures devices. (A colour version of this figure can be viewed online.)

$1.84 \times 10^{-3} \times \frac{hc}{q(\mu_p \tau_{e-p} + \mu_n \tau_{e-n})}$, and $1.42 \times 10^{-3} \times \frac{hc}{q(\mu_p \tau_{e-p} + \mu_n \tau_{e-n})}$, respectively.

According to Eq. (27), the binding energy is correlated by the applied electric field because $E_B \propto -q(\mu_p \tau_{e-p} + \mu_n \tau_{e-n})F^2$. Using the expression of the maximum electric field in the channel of Eq. (41), we can find that the binding energy obeys a 2 order polynomial relation with the source-drain voltage and the source-gate voltage. Fig. 8 depicts how the trion binding energy in photoluminescence spectra of the MoS_2/graphene heterostructure changes with the gate voltage. Experimental data in Fig. 8 come from Fig. 3c in Ref. [22]. This figure clearly demonstrates that the proposed model agrees well with the experimental data. The fitting parameter C_2 is $-2.38 \times 10^{-3} \times \frac{hc}{q(\mu_p \tau_{e-p} + \mu_n \tau_{e-n})}$.

Eqs. (43) and (44) clearly show that the peak energy in the emission (absorption) spectrum for field-effect transistors increases with the increased source-drain voltage and source-gate voltage when $C_3 \leq \frac{1}{L} V_{DS} + \frac{L}{\lambda^2} V_{GS}$, whereas the peak energy decreases with the increased source-drain voltage and source-gate voltage when $C_3 \geq \frac{1}{L} V_{DS} + \frac{L}{\lambda^2} V_{GS}$. In other words, the absorption and emission spectrum can be shifted to higher energy or lower energy by tuning source-drain voltage and source-gate voltage. The correlation between the shift and the source-drain (gate) voltage still obeys a 2 order polynomial dependent relation according to Eq.43. Additionally, one can note that $C_2 \approx -\frac{L\varepsilon_{ox}}{\varepsilon_s t_s t_{ox}}$, which represents the C_2 fitting parameter depends on the channel length and the oxide thickness. Therefore, the large variation of the C_2 fitting parameters in all graphene related electronic devices obtained in this paper could origins from the large variation in the channel length and the oxide thickness.

4. Conclusions

We have theoretically investigated the energy relaxation of the excitons in graphene related electronic devices based on the ambipolar transport theory. Thus an analytical physical model of

the impacts of the source-gate voltage and the source-drain voltage on in the spectral shifts in graphene related electronic devices has been proposed based on the energy conservation equation with the balance assumption. The energy relaxation of the excitons can result that the exciton can get energy from an applied electric field, thus a shift in the emission (absorption) spectrum will occur. The validity of propose model has been checked by comparing the predicted results with experimental data reported in Refs. [21–26]. Those experimental data clearly demonstrate that the proposed model is good to describe the gate voltage dependent and drain voltage dependent spectral shift. We predict that the changes in the spectral shift depends on the channel length, the gate oxide thickness, the dielectric constant of the gate oxide, the thickness of the graphene layer, and the dielectric constant of the graphene for graphene related electronic devices. All these physical parameters could affect electrostatic tunability of optical transitions for the gate control of the spectral shift. On the other hand, only changing channel length has a main contribution to the drain control of the spectral shift. Further, electric field dependent spectral shape of the absorption and emission spectra in graphene related electronic devices can be predicted by using the proposed model (Eq. (27), (30), and (40)). Physical model of tuning of the absorption wavelength and emission wavelength via gate modulation or drain modulation can help us to understanding the continuous tuning mechanism. Our model of the continuous wavelength tuning in graphene related electronic devices not only represents a method for the absorption and emission wavelength tuning but also an important possibility to optimize future light-emitting devices and light detector by using its physical parameters.

Acknowledgment

The authors acknowledge financial support from the National Natural Science Foundation of China, grant Nos. 61076102 and 61471035, and the Fundamental Research Funds for the Central Universities under Grant Nos. 06500010 and 06105031.

References

[1] E. Riccardi, M.A. Méasson, M. Cazayous, A. Sacuto, Y. Gallais, Gate-dependent electronic Raman scattering in graphene, Phys. Rev. Lett. 116 (6) (2016) 066805.
[2] C. Chakraborty, L. Kinnischtzke, K.M. Goodfellow, R. Beams, A.N. Vamivakas, Voltage-controlled quantum light from an atomically thin semiconductor, Nat. Nanotechnol. 10 (6) (2015) 507–511.
[3] F. Jakubka, S.B. Grimm, Y. Zakharko, F. Gannott, J. Zaumseil, Trion electroluminescence from semiconducting carbon nanotubes, ACS Nano 8 (8) (2014) 8477–8486.
[4] C.F. Chen, C.H. Park, B.W. Boudouris, J. Horng, B. Geng, C. Girit, et al., Controlling inelastic light scattering quantum pathways in graphene, Nature 471 (7340) (2011) 617–620.
[5] F. Wang, Y. Zhang, C. Tian, C. Girit, A. Zettl, M. Crommie, Y.R. Shen, Gate-variable optical transitions in graphene, Science 320 (5873) (2008) 206–209.
[6] J.S. Ross, S. Wu, H. Yu, N.J. Ghimire, A.M. Jones, G. Aivazian, et al., Electrical control of neutral and charged excitons in a monolayer semiconductor, Nat. Commun. 4 (2013) 1474.
[7] S. Schwarz, A. Kozikov, F. Withers, J.K. Maguire, A.P. Foster, S. Dufferwiel, et al., Electrically pumped single-defect light emitters in WSe2, 2D Mater. 3 (2016) 025038.
[8] L.F. Mao, H. Ning, J.Y. Wang, The current collapse in AlGaN/GaN high-electron mobility transistors can originate from the energy relaxation of channel electrons, PloS one 10 (6) (2015) e0128438.
[9] L.F. Mao, H. Ning, Z.L. Huo, J.Y. Wang, Physical modeling of gate-controlled Schottky barrier lowering of metal-graphene contacts in top-gated graphene field-effect transistors, Sci. Rep. 5 (2015) 18307.
[10] L.F. Mao, H. Ning, C. Hu, Z. Lu, G. Wang, Physical modeling of activation energy in organic semiconductor devices based on energy and momentum conservations, Sci. Rep. 6 (2016) 24777,.
[11] W. Van Roosbroeck, The transport of added current carriers in a homogeneous semiconductor, Phys. Rev. 91 (2) (1953) 282–289.
[12] C.L. Tien, A. Majumdar, F.M. Gerner, Microscale Energy Transport, Taylor & Francis, Washington, DC, USA, 1998.
[13] N.A. Amin, Z. Johari, M.T. Ahmadi, R. Ismail, Low-field mobility model on parabolic band energy of graphene nanoribbon, Mod. Phys. Lett. B 25 (04) (2011) 281–290.
[14] M.S. Sodha, D.P. Tewari, J. Kamal, H.D. Pandey, A.K. Agarwal, V.K. Tripathi, Nonlinear mechanisms for self-focusing of microwaves in semiconductors, J. Appl. Phys. 44 (4) (1973) 1699–1705.
[15] M. Meyyappan, T.R. Govindan, Radio frequency discharge modeling: moment equations approach, J. Appl. Phys. 74 (4) (1993) 2250–2259.
[16] V. Kolobov, R. Arslanbekov, Deterministic Boltzmann solver for electron kinetics in plasma reactors for microelectronics applications, Microelectron. Eng. 69 (2) (2003) 606–615.
[17] D. Jena, A theory for the high-field current-carrying capacity of one-dimensional semiconductors, J. Appl. Phys. 105 (12) (2009) 123701.
[18] T. Numai, Optical transitions, in: Fundamentals of Semiconductor Lasers, Springer, Japan, 2015, pp. 23–40.
[19] K.K. Young, Short-channel effect in fully depleted SOI MOSFETs, IEEE Trans. Electron Dev. 36 (2) (1989) 399–402.
[20] S.H. Lee, Y.S. Yu, S. Hwang, D.A. Ahn, SPICE-compatible new silicon nanowire field-effect transistors (SNWFETs) model, IEEE Trans. Nanotechnol. 8 (5) (2009) 643–649.
[21] X. Wang, H. Tian, M.A. Mohammad, C. Li, C. Wu, Y. Yang, T.L. Ren, A spectrally tunable all-graphene-based flexible field-effect light-emitting device, Nat. Commun. 6 (2015) 7767.
[22] Y. Li, C.Y. Xu, J.K. Qin, W. Feng, J.Y. Wang, S. Zhang, et al., Tuning the Excitonic States in MoS2/Graphene van der Waals Heterostructures via Electrochemical Gating, Adv. Funct. Mater 26 (2) (2016) 293–302.
[23] M. Copuroglu, P. Aydogan, E.O. Polat, C. Kocabas, S. Sưzer, Gate-tunable photoemission from graphene transistors, Nano Lett. 14 (5) (2014) 2837–2842.
[24] M. Steiner, M. Freitag, V. Perebeinos, A. Naumov, J.P. Small, A.A. Bol, P. Avouris, Gate-variable light absorption and emission in a semiconducting carbon nanotube, Nano Lett. 9 (10) (2009) 3477–3481.
[25] M. Freitag, M. Steiner, A. Naumov, J.P. Small, A.A. Bol, V. Perebeinos, P. Avouris, Carbon nanotube photo-and electroluminescence in longitudinal electric fields, ACS Nano 3 (11) (2009) 3744–3748.
[26] K.T. Nguyen, D. Abdula, C.L. Tsai, M. Shim, Temperature and gate voltage dependent raman spectra of single-layer graphene, ACS Nano 5 (6) (2011) 5273–5279.